Journal of Power Sources, 27 (1989) 45 - 58

CURRENT DISTRIBUTION IN LEAD/ACID AND NICKEL/CADMIUM ACCUMULATORS

J. MEIWES and H.-CH. SKUDELNY

Institute for Power Electronics and Electrical Drives, Aachen University of Technology, Aachen (F.R.G.)

(Received July 14, 1988; in revised form February 2, 1989)

Summary

A simple method of determining the current distribution in accumulators which keeps the measuring and computational requirements within practical limits is briefly described. The local maximum and minimum loading conditions within the battery can be obtained with satisfactory accuracy.

The current distributions in different types of lead/acid and nickel/cadmium accumulator were investigated. It depends on a number of parameters; discharge current, state-of-discharge, construction type, type of system and temperature. These were investigated and the result discussed. We also highlighted the differences encountered in the behaviour of the current distribution in lead/acid and alkaline accumulators.

Introduction

High performance accumulators require a uniform utilisation of the electrodes, *i.e.*, a homogeneous current distribution*. Voltage drops, however, cause inhomogeneities resulting in position-dependent 'local' discharge states which are notably larger than the 'global' state-of-discharge associated with the total battery current, especially at the top of the battery.

A non-uniform current distribution is not desired; the resultant local state-of-discharge limits the amount of energy which can be drawn and significant energy reserves within the battery cannot be utilised [1]. In addition, excessive local discharges reduce the battery life.

There are various reasons for the current distribution being inhomogeneous, each having different consequences. The investigations conducted consider the influence of the longitudinal voltage drops within the electrodes on the distribution of the transverse current density. They lead to an under-

*All voltages, currents and current densities are the transverse values in the cell (*i.e.*, across the electrolyte) unless specified differently.

0378-7753/89/$3.50 © Elsevier Sequoia/Printed in The Netherlands

standing of the dependence of the current distribution on the following parameters; discharge current, state-of-discharge, temperature, height of battery, construction type and type of system. At the same time they also enable remedial measures to be evaluated.

Method of investigation

The current distribution is determined by measuring the voltage between the positive and the negative electrodes at several points and then deriving the transverse current densities.

Since such a model for determining the current distribution from the given voltages is not very accurate, other factors, such as minute temperature fluctuations, have to be considered. Determination of the current density is assisted by the fact that there is a position in the battery — typically just above the centre of the plate — where the local current density corresponds very closely to the average current density over the complete discharge. Thereby, a general 'representative' relationship is obtained between the transverse voltages and the transverse current density which is valid if the current density is constant or is only changing slowly.

$$u_{q,\,rep} = f_{u,\,rep}(q_{loc,\,rep}, j_{q,\,rep}) = f_{u,\,rep}(q_B, i_B) \tag{1}$$

The use of the above equation on the transverse voltages measured at other points within the battery enables the relevant current densities to be determined.

The easiest way is to consider only the largest and smallest current densities at the top and bottom of the electrodes together with the average value at the beginning of the discharge. If, therefore, the transverse voltages are measured at three points (at the top, just above the centre and at the bottom), two different discharge currents, the maximum and minimum current densities can be determined using a simple graphical method [2].

A more rigorous approach is to derive the current distribution from measurements of voltages at many points in a series of constant-current discharge tests. This enables the distribution of the current density over a range of discharge rates to be determined.

It is also possible, that with detailed monitoring, the mechanism involved in local losses may be better understood.

In addition, unavoidable measuring errors can be detected and in some cases, compensated for. The measuring and computational requirements, however, are extensive [2, 3].

Our approach is a compromise between the briefly described alternatives. Since the measuring and computational requirements stay within practical limits, and since the most important results concerning the current distribution can be obtained with significant accuracy, this approach is especially suited for analytical purposes. It is necessary, however, that the points of maximum and minimum current density are known. This can be

from criteria with similar types of cell [3, 4], or from a knowledge of the geometry of the plate grid as well as the position of the terminal lugs.

For batteries, in which the height of the plate exceeds the width, a one-dimensional analysis of the vertical dependence of the current distribution is permitted. Voltages differences across the plates are negligible. The voltages at the top and bottom of the electrodes (the points where the largest deviations from the average current are found) are measured during the course of at least two constant-current discharge tests. The measurement of the representative transverse voltage can be omitted, if the characteristic pattern of the voltage drops within the plates is known. This representative voltage can then be calculated from the voltages of the top and bottom of the plate using an averaging technique which takes into consideration the pattern of the voltage drops.

With uniform electrodes and a fully charged battery, the difference between the relaxation voltage and the local transverse voltage is estimated to be an exponential function of the height of the battery. Thus, a geometrical mean is conveniently used as a first order approximation to calculate the representative transverse voltage

$$u_{q,\,rep*} = u_{q,\,top} + (u_{q,\,bottom} - u_{q,\,top}) \times f \qquad (2)$$

$$\text{where} \quad f = \frac{\sqrt{(u_0 - u_{q,\,top})(u_0 - u_{q,\,bottom})}}{u_{q,\,bottom} - u_{q,\,top}}$$

The factor f is determined at the beginning of the discharge and used then throughout to determine the representative transverse voltage (u_0 is the relaxation voltage of a fully charged battery). In each case the acceptability of this first order approximation must be checked, otherwise the calculations have to be derived from the exact results obtained by using the transmission line circuit model [5, 6].

In the following, the compromise approach is used to see how the current densities behave at those points within the battery, at which the voltages deviate by an amount, Δu. The behaviour of the representative voltage — under a constant-current discharge — is described by eqn. (3) which is based on the equivalent circuit shown in Fig. 1.

$$u_{q,\,rep}(i_B, q_B) = u_0(i_B, q_B) - j_{q,\,rep} \times r(i_B, q_B) - q_{loc,\,rep}/c(i_B, q_B) \qquad (3)$$

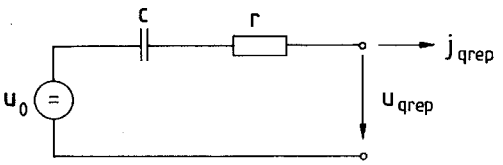

Fig. 1. Simple equivalent circuit diagram for the representative voltage for constant or almost constant discharge currents.

The operating point dependent parameters — the ideal voltage source u_0, the internal capacitance c and the internal resistance r — are only changing slowly and for short periods of time can be assumed to be constant. In addition, the representative current density and the local state of discharge can be identified by the battery current and the global state of discharge. The following relationship is valid for the representative local area

$$u_{q,\,rep}(i_B, q_B) = u_0 - q_B/c - i_B \times r \tag{4}$$

For other local areas with the time dependent voltage, $u_q(t)$, at these points and the transverse current density, $j_q(t)$, we get

$$u_0 - u_q(t) = 1/c \int_0^t j_q(t) \times dt + j_q(t) \times r \tag{5}$$

Solving this equation for the deviations from the representative voltages, leads to the following equation

$$\Delta u_q = -\Delta j_q r - \Delta q_{loc}/c \tag{6}$$

where $\Delta u_q = u_{q,\,rep} - u_q$; $\Delta j_q = j_{q,\,rep} - j_q$; $\Delta q_{loc} = q_{loc,\,rep} - q_{loc}$.

This can be represented by the equivalent circuit diagram shown in Fig. 2, where $\Delta u_q(t)$ corresponds to the longitudinal voltage drop within the plates and is determined by the battery current and the longitudinal resistance. By means of $\Delta j_q(t)$, the difference between the current density at the top and bottom of the plates can be derived.

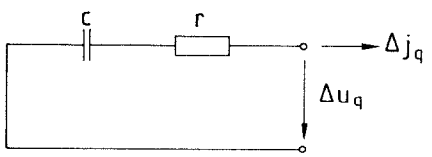

Fig. 2. Simplified equivalent circuit diagram valid for deviations from the conditions at the representative point.

Thus, the current densities at the top and the bottom of the plates can be calculated. As far as Δj_q is concerned, the internal capacitance, c, and the internal resistance, r, are decisive. At the start of the discharge ($q_B = 0$), Δj_q is an inverse function of the internal resistance. If r and c are both constant, the battery current with its time constant, rc, assumes on the mean or representative current density and remains unchanged thereafter. The remaining difference in the state-of-discharge is then given by $-\Delta u_q c$. Constant values for both r and c, however, can only be assumed over a limited area. The internal resistance and capacitance can be derived from the measured representative voltages of at least two constant-current discharge tests using the following equations

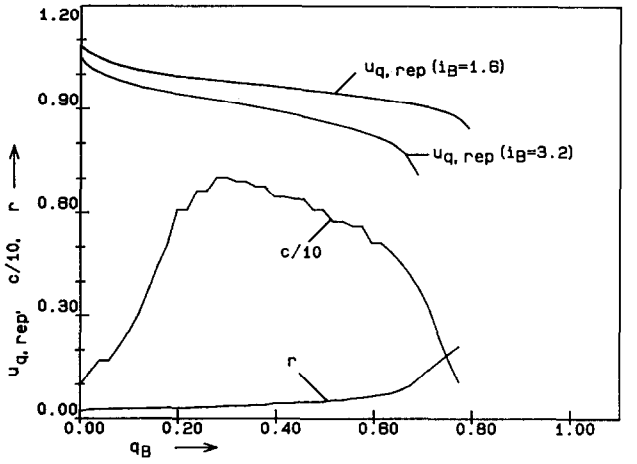

Fig. 3. Representative voltage of a nickel/cadmium accumulator type H 203 with fibre-structured electrodes during two constant-current discharges of $i_B = 1.6$ and 3.2, as well as the internal capacitance and resistance (eqn. (7)) all plotted *vs.* the state of discharge.

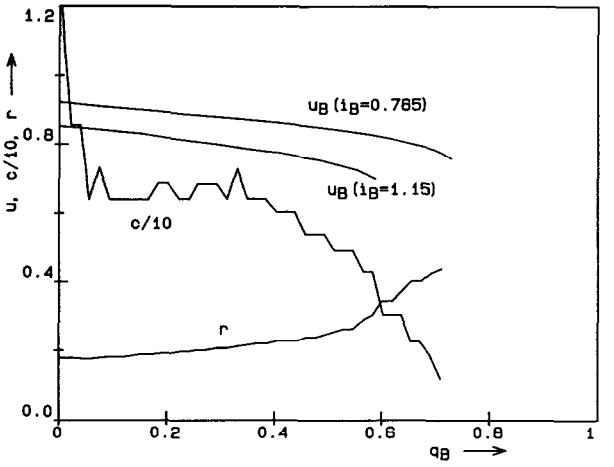

Fig. 4. Representative voltage of a lead/acid accumulator type 3 PzS 360 tubular plates during two constant-current discharges of $i_B = 0.765$ and 1.15, as well as the internal capacitance and resistance all plotted *vs.* the state of discharge.

$$c(i_B, q_B) = (du_{q,rep}(i_B, q_B)/dq_B)^{-1}$$
$$r(i_B, q_B) = du_{q,rep}(i_B, q_B)/di_B \qquad (7)$$

Figures 3 and 4 shows the characteristic behaviour of $u_{q,rep}$, c and r, for a nickel/cadmium and lead/acid accumulator during discharge.

Typically, the internal resistance of both lead/acid and alkaline accumulators only changes slightly at the beginning of the discharge and

increases towards the endpoint. The internal capacitance variations between the two types of accumulator system, however, differ significantly [7, 8].

In lead/acid accumulators c remains approximately constant for mean discharge states and rapidly decreases if discharging is continued. At the beginning of discharge a very large or negative c is possible due to numerical instabilities.

In contrast, the internal capacitance of alkaline accumulators is very small at the beginning of the discharge and typically increases to higher values, than in lead/acid accumulators for discharge states of between 10 and 15%. This large internal capacitance is then maintained, until shortly before the endpoint is reached when it drops to a very small value.

The time constant obtained by r and c can range from a few minutes up to two hours for both types of accumulator systems.

This behaviour of the internal capacitance and resistance determines the local deviations of the current density, from the mean current density, Δj_q. By using eqn. (6), the value of Δj_q can be determined numerically. Figure 5 shows for instance the current density at the top and bottom of the electrodes *versus* the state of discharge for a nickel/cadmium accumulator with the characteristics shown in Fig. 3.

For alkaline accumulators Δj_q, typically, has a maximum value at the beginning of the discharge. The differences in the current densities then decrease until a state-of-discharge, $q_B = 0.1$ to 0.15 is reached after which they decrease only a little and may even temporarily increase again.

From discharge states of $q_B = 0.2$ onwards, j_q typically varies more slowly than in lead/acid accumulators. Just before the discharge endpoint is reached, Δj_q becomes zero, then increases rapidly in the reverse direction during the final state of discharge.

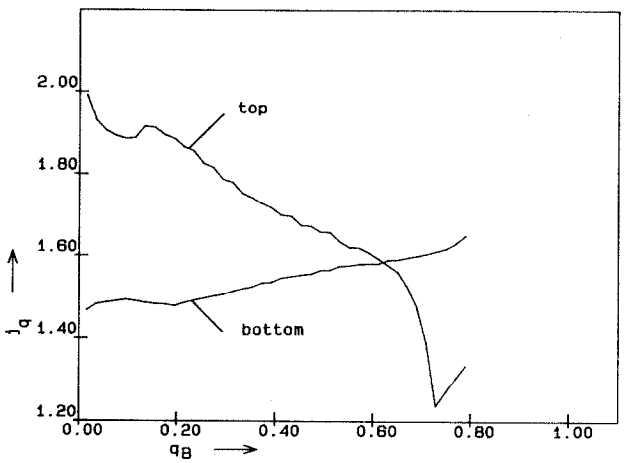

Fig. 5. Current densities at the top and bottom of the electrodes at a discharge current of $i_B = 1.6$, *vs.* the state of discharge (corresponds to Fig. 3).

Measuring results

The following results were either obtained using the complete approach or the comprise, described above, when it gave results which only differed negligibly from those obtained using the complete approach.

The terminal voltage, the local voltages at the top and bottom of the electrodes and the representative voltage were all monitored. Figures 6 and 7 show these voltages for various constant-current discharges. It is apparent that for both types of battery, there is very little difference between the individual curves of any one set at a given discharge current. To a first order approximation, the difference between the voltage curves of the top and bottom of the electrodes increases linearly with the discharge current, since they are caused by the, almost constant, longitudinal resistance.

The current densities at the top and bottom of the electrodes were calculated from the test results shown in Figs. 6 and 7.

Figures 8 and 9 show the current densities at these two points *versus* the state-of-discharge for various values of constant-current discharge.

Figure 8 refers to a high-current type of cell with fibre-structured electrodes. It can be seen that the difference in current between the top and the bottom of the electrodes is negligible at small discharge currents ($i_B = 0.2$).

For medium and large discharge currents, two typical characteristics of the current distribution profiles of alkaline accumulators can be recognised.

Firstly, the differences in the current densities are largest at the beginning of discharge and initially decrease very rapidly until the state of

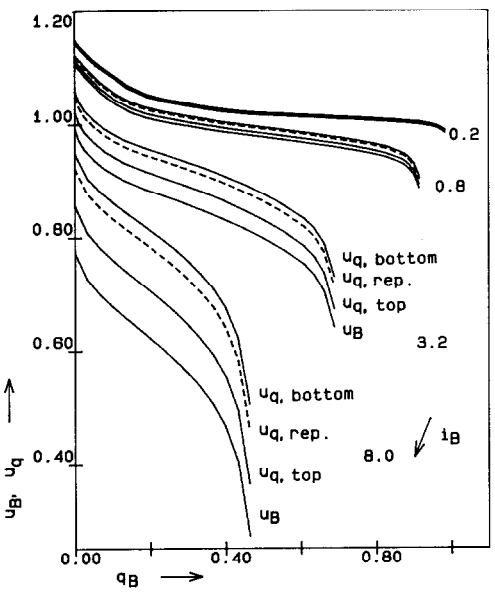

Fig. 6. Local voltages and the terminal voltages of a nickel/cadmium accumulator with fibre-structured electrodes of the high-current type (H 203) *vs.* the state-of-discharge for various values of discharge currents.

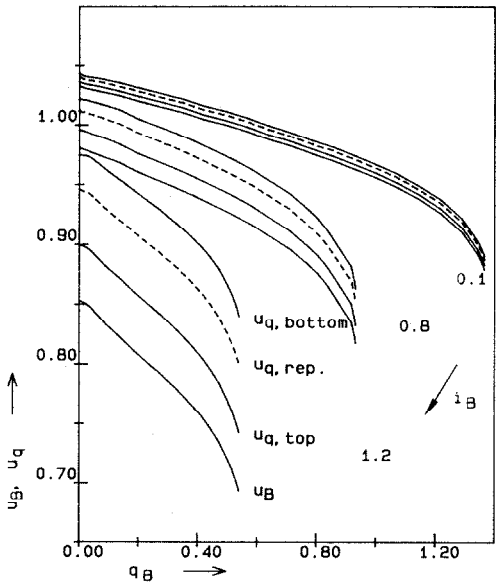

Fig. 7. Local voltages and the terminal voltage of a lead/acid accumulator with tubular plates (type 3 PzS 360) *vs.* the state-of-discharge for various values of constant-current discharge.

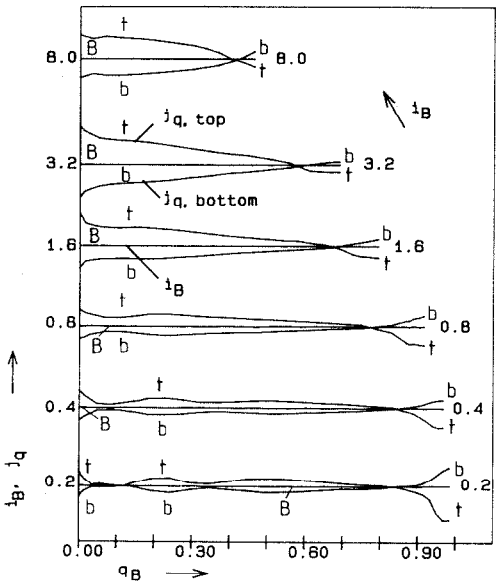

Fig. 8. Local current densities at the top and bottom of the electrodes of a nickel/cadmium accumulator with fibre-structured electrodes of the high-current type H 203 *vs.* the state-of-discharge for various values of discharge currents (t = top, b = bottom, B = battery).

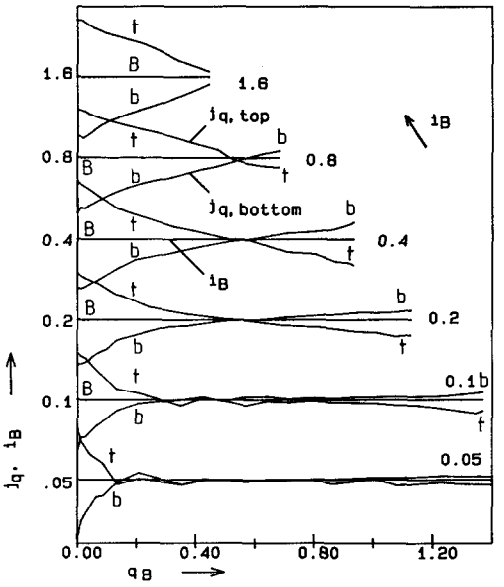

Fig. 9. Transverse current densities at the top and bottom of the electrodes of a lead/acid accumulator with tubular plates of the type 3 PzS 360 *vs.* the state-of-discharge for various values of discharge currents (t = top, b = bottom, B = battery).

discharge reaches $q_B = 0.1$. During this period the voltage (Fig. 6), drops exponentially. When the voltage has stabilised, the current distribution varies less rapidly.

Secondly, for mean currents, the differences in the current distribution may temporarily increase. Unlike lead/acid accumulators, the currents are only the same over the whole of the cell area when the terminal voltage begins to collapse, approximately 15% before the endpoint of discharge is reached. The delayed equalisation of the current distribution is related to the independence of the terminal voltage on the state of discharge for mean relative discharge states.

When the terminal voltage collapses the profile of the current distribution reverses. Only qualitative statements can, however, be made, since there are larger measuring errors at this stage. The dependence of the terminal voltage on the state-of-discharge at this operating point is significant. Thus, small inhomogeneities in the electrodes or transverse resistances, can influence the voltage drops within the plates considerably. The method used to determine the current distribution, however, presupposes homogeneous transverse resistances for a constant load.

Figure 9 shows the current densities of the top and bottom of the electrodes of a lead/acid accumulator with tubular plates (type 3 PzS 360) *versus* the state-of-discharge for various constant-current discharges. It is seen, that the difference in current density is largest at the beginning of the discharge. In contrast to alkaline accumulators, the inhomogeneity continu-

ously decreases, until the current distribution at a state of discharge of $q_B = 0.5$ to 0.7 is largely equalised. The statement, that the transverse current density is equalised at this mean state-of-discharge, was found to be valid for all lead/acid accumulators investigated over the entire range of constant-current discharges. Continued discharging leads to a reversal in the current distribution profiles, although, at the endpoint of discharge, the differences are still smaller than at the beginning of the discharge. At very large discharge currents ($i_B > 1.6$) there is no reversal of the current distribution profile, because the endpoint of discharge is reached prematurely.

With very small currents (e.g. $i_B = 0.05$), an uneven current distribution is only observed at the beginning of the discharge: it becomes equalised at a state-of-discharge of $q_B = 0.2$. The small difference in the local state-of-discharge between the top and the bottom of the cell, is then sufficient to reduce the voltage and tends to maintain the equalised current distribution until the endpoint is reached.

The profiles of the current density and the local discharge states both exhibit a similar characteristic pattern. The integral of the difference between the current densities at the top and bottom of the electrodes and the battery current results in the local state of discharge which is of special interest. Since the determination of the current distribution when the voltage collapses in alkaline accumulators is not accurate, the following comparison between the local discharge states is not conducted at the endpoint of discharge, but when the current is homogeneous — typically 85% discharged.

Figure 10 shows the comparison between the local discharge states for various different types of alkaline accumulator. It is seen, that the relative differences in the local discharge state almost disappear for small discharge currents of $i_B < 0.5$. The differences, however, increase with increasing discharge currents up to $i_B = 3$, after which the rate of increase is reduced. This increase is mainly caused by a decline in the charge which can be drawn, since the absolute differences in the local-discharge-state-current just before the endpoint for a large discharge, are almost independent of the current.

The differences in the local discharge states are not significant for the high-current (H 303) and the low-current (L 302) accumulators with pocket plates.

For batteries with fibre-structured electrodes the ratios are different. With these, the differences in the local discharge states are larger for the low-current type (L202) than for the high-current type (H203). This leads to the conclusion that the longitudinal resistances of the high-current type were decreased more than the transverse resistances, in comparison to the low-current type.

To compare the inhomogeneity of the current distribution for different types of construction, the individual heights of the plates have to be considered. Theoretically, the relationship between the inhomogeneity of the current distribution and the physical height of a battery is a hyperbolic function [6]. The heights considered here, however, are small enough to permit us to assume a linear relationship.

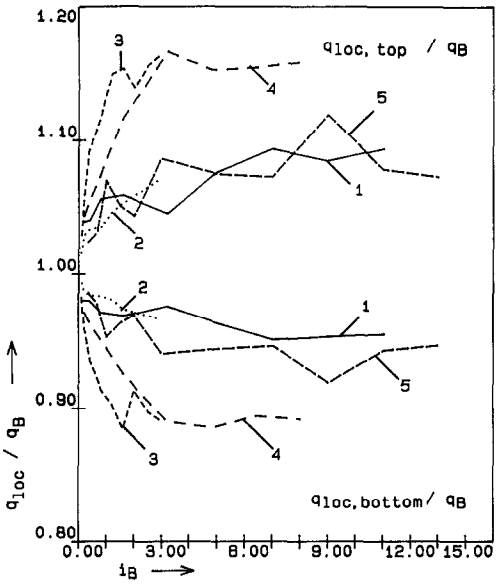

Fig. 10. Ratio of the maximum and minimum local discharge state to the global discharge state for various types of alkaline accumulators *vs.* the battery current at about the 85% discharge state (the point where the current is homogeneous, or where the largest differences in the local discharge state are found).

No.	Type	Manufacturer	K_n (A h)	Plate height (cm)	Comment
1	H 303	SAB Nife	32.0	20	pocket plate
2	L 302	SAB Nife	102.0	20	pocket plate
3	L 202	Hoppecke	40.4	16	fibre-struct.
4	H 203	Hoppecke	30.0	16	fibre-struct.
5	VS 410 X	Varta AG	30.0	10	sintered plate

Normalising the curves shown in Fig. 10 for the pocket plate accumulators plate height increases the difference in the local discharge states for the fibre-structured accumulators about 30%, for the sintered plate accumulator about 100%.

Consequently, the sintered plate types at the beginning of the discharge have the largest inhomogeneities. This accumulator, though, also provides the largest discharge currents. The relatively large inhomogeneities of the fibre-structured accumulators are linked to the small internal resistances characteristic for this type of accumulator.

The measured local discharge state pattern of lead/acid accumulators differs from that of alkaline accumulators. Figure 11 shows the ratio of the maximum and minimum discharge states to the global discharge state at the endpoint of discharge *versus* the discharge current for various types of lead/acid accumulator. The difference between the top and bottom of the cell

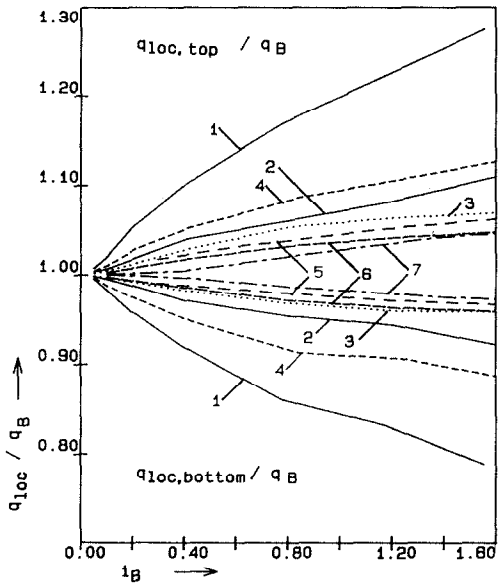

Fig. 11. Ratio of the maximum and minimum local discharge states to the global discharge state at the endpoint of discharge (0.3 V below the initial voltage) for different types of batteries at room temperature. Manufacturer: HAGEN Batterie A.G.

No.	Type	K_n (A h)	Plate height (cm)	Comment
1	3 PzS 360	360.0	54	
2	3 PzS 210	210.0	31	
3	3 PzS 210	210.0	31	opposite terminal lugs
4	3 CSM 435	435.0	54	copper stretch metal battery
5	3 Ps 190	112.5	19	30 °C
6	5 PzF 175	175.0	19	
7	Starter battery	44.0	12	manufacturer: Ford motor-craft

increases with the longitudinal resistance, *i.e.*, as the height of the cell — of a given construction type — increases. Furthermore, the relative differences increase as the discharge current increases, resulting in a reduced available capacity. As can be seen from Fig. 11, the difference in the case of the type 3 PzS 360 is about 2.5 times larger than that of the type 3 PzS 210; the latter being similar to the copper mesh metal battery. For small electric vehicle starter batteries, e.g. the type 5 PzF 175, and starter batteries the maximum local discharge state towards the endpoint of discharge for battery currents of $i_B = 1.6$ is about 5% above the global state of discharge. For average discharge currents of $i_B = 0.5$, the difference is about 2.5%.

In addition to cell height, temperature also effects the current distribution by changing the transverse resistances. In contrast the longitudinal resistances of the metallic conductors are comparatively independent of

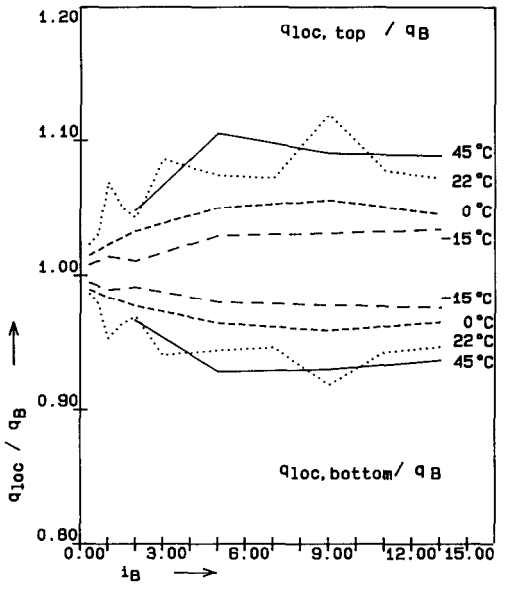

Fig. 12. Ratio of the maximum and minimum local discharge states to the global discharge state of a sintered plate accumulator (type VS 410 X) just before the endpoint of discharge is reached (the point with the largest differences in the local discharge states) *vs.* the battery current for various temperatures.

temperature. Thus, the current should be more homogeneous at low temperatures than at high ones. Figure 12 shows how the relative differences in the local discharge states of a sintered plate accumulator compare for various temperatures. As the temperature is increased from −15 °C the difference in the local discharge states between top and bottom of the cell increases up to 22 °C. Between 22 and 45 °C the difference is hardly significant.

Conclusion

The described metering method for the current distribution in accumulators is qualified for constant current discharges. The metering results give an overview over the current distribution and its dependence on a number of parameters. It is possible to compare a lot of similar accumulators directly with these results.

Acknowledgements

We thank the 'Deutsche Forschungsgemeinschaft (DFG)' for supporting this study and the respective manufacturers for supplying the batteries.

List of Symbols

$U_n = 2$ V	rated voltage of lead/acid accumulators
$U_n = 1.2$ V	rated voltage of nickel/cadmium accumulators
$K_n = K_5$	rated capacity
$T_n = 1$ h	reference time
$I_n = K_5/T_n$	reference current
$R_n = U_n/I_n$	reference resistance
A_n = total area of separators = reference cross-section	
$J_n = I_n/A_n$	reference current density

From the above, the following relative quantities are derived and denoted by lower case letters.

$u = U/U_n$	relative voltage
$t = T/T_n$	relative time
$i = I/I_n$	relative current
$r = R/R_n$	relative resistance
$j = J/(I_n/A_n)$	relative current density

$q_B = \int_0^t i_B \, dt$ state of discharge; $q_B = 0$ for fully charged batteries

$q_{loc} = \int_0^t j_q \, dt$ local state of discharge.

Indices

loc	local
rep	representative
q	transverse
B	battery

Other symbols

f	factor, function

References

1 W. G. Sunu and B. W. Burrows, *J. Electrochem. Soc., 128* (1981) 1405 - 1411.
2 J. Meiwes, *Elektrotech. Z. Archiv, 8* (3) (1986) 79 - 85.
3 J. Meiwes, Untersuchungen zur Stromverteilung in Akkumulatoren, *Doctor thesis*, Aachen University of Technology, F.R.G.
4 J. Meiwes, *Elektrotech. Z. Archiv, 8* (9) (1986) 305 - 312.
5 J. Euler and L. Horn, *Archiv. Elektrotech. (Berlin), 50* (2) (1965) 85 - 90.
6 J. Meiwes, *Elektrotech. Z. Archiv, 7* (12) (1985) 381 - 387.
7 H. Bode, *Lead–Acid Batteries*, Wiley, New York, 1977.
8 S. U. Falk and A. J. Salkind, *Alkaline Storage Batteries*, Wiley, New York, 1969.